Microchimica Acta (2021) 188: 351
https://doi.org/10.1007/s00604-021-05008-4

ORIGINAL PAPER

Metal–organic framework modified by silver nanoparticles for SERS-based determination of sildenafil and pioglitazone hydrochloride

Yanru Ding[1] · Yuqi Cheng[1,2] · Baoqin Hao[1] · Lin Zhu[3] · Nan Zhang[1] · Bing Zhao[3] · Yuan Tian[1]

Received: 24 May 2021 / Accepted: 26 August 2021 / Published online: 23 September 2021

Abstract

A versatile surface-enhanced Raman scattering (SERS) assay has been established that can realize rapid and sensitive determination of sildenafil (SIL) and pioglitazone hydrochloride (PIO) adulteration in healthcare products. Metal–organic frameworks-silver nanoparticles (MOFs-AgNPs) with SERS activity were successfully prepared via in situ synthesis AgNPs on the MOFs surface. By virtue of the adsorptivity of MOFs, the MOFs-AgNPs could effectively concentrate the drug molecules on the electromagnetic enhancement areas of AgNPs. Moreover, the MOFs-AgNPs substrate exhibited more sensitive SERS activity than classical AgNPs with linear range of 1.0×10^{-7}–1.0×10^{-5} mol L^{-1} for SIL and 8.0×10^{-7}–3.0×10^{-5} mol L^{-1} for PIO and limit of detection (LOD) of 4.8×10^{-8} mol L^{-1} for SIL and 1.4×10^{-7} mol L^{-1} for PIO. The designed method realized the determination of SIL and PIO in commercial tablets and healthcare products with recoveries of 93.8–108.0% and 93.0–104.0%, respectively, with relative standard deviation (RSD) of 2.7–4.1% and 2.2–4.2%, respectively. The present system displayed little interference effect on determination. This work provides a multifunctional route for the determination of other drugs via the SERS technology.

Keywords Surface-enhanced Raman scattering · MOFs-AgNPs · Sildenafil · Pioglitazone hydrochloride · Healthcare products

Introduction

Sildenafil (SIL), a type of phosphodiesterase type 5 inhibitor, has an effect on treating male erectile dysfunction and alleviation of pulmonary hypertension [1]. However, common side effects such as headache, flushing, indigestion, visual abnormalities, and decreased blood pressure overlap may occur after taking the drug [2]. Pioglitazone hydrochloride (PIO), am oral antihyperglycemic agent, is suitable for the treatment of type-2 diabetes. Improper dosage or overdose of PIO will increase the risk of bladder cancer [3]. These drugs are considered prescription and must be administrated under the guidance of the doctor. In view of the low side effects of health products and regulation of human body functions, some manufacturers have illegally added chemical drugs to various health products to demonstrate high efficiency and immediate effect [4]. According to the relevant regulations, the addition of drugs in food or healthcare products is prohibited. Once the SIL and PIO are illegally adulterated to health products, consumers may be at risk of kidney and liver damage for long time ingest. With this regard, determining whether healthcare products are illegally added with SIL and PIO is urgently needed.

At present, the researches for determining SIL and PIO mainly include electrochemical assay [5, 6], ultraviolet spectrophotometric assay [7], high-performance liquid chromatography assay (HPLC) [8, 9], thin layer chromatography-surface-enhanced Raman spectroscopy assay (TLC-SERS)

✉ Yuan Tian
tianyuan@jlu.edu.cn

1 College of Chemistry, Jilin Province Research Center for Engineering and Technology of Spectral Analytical Instruments, Jilin University, Changchun 130012, People's Republic of China

2 State Key Laboratory of Supramolecular Structure and Materials, Institute of Theoretical Chemistry, College of Chemistry, Jilin University, Changchun 130012, People's Republic of China

3 State Key Laboratory of Supramolecular Structure and Materials, Jilin University, Changchun 130012, People's Republic of China

[10, 11], fluorescence assay [12], liquid chromatography-mass spectrometry assay (LC-MC) [13], LC-MC/MC [14], and SERS[15–17]. These analytical methods employed to realize high sensitivity and accurate determination. For example, HPLC allows to separate and analyze multiple components simultaneously. Electrochemical assay can rapidly obtain the composition of complex system, fluorescence shows high sensitivity, and ultraviolet spectrophotometric has wide application field. However, they also have certain drawbacks. For example, the operation of HPLC is relatively time-consuming, and fluorescence may suffer from photobleaching. And the quantitative determination of TLC is not ideal. Thus, developing a rapid and sensitive approach to detect chemical drugs in illegally added natural health products is significant.

SERS, with the merits of high sensitivity, nondestructive testing, and characteristic "fingerprint" properties, has been widely used in the field of chemical and biological analysis as a powerful analysis technology [18, 19]. The excellent SERS performance depends on the use of SERS substrate with strong local surface plasmon resonance (LSPR) and high affinity toward target molecules. Unfortunately, many drug molecules have small Raman scattering cross section and low affinity with the nanoparticles, making them exhibit low Raman activity or no SERS signal generation. On the other aspect, the major shortcomings of in employing classical sliver nanoparticles (AgNPs), involving in easy aggregation and poor stability, may certainly limit their sensitivity and reproducibility in SERS area. Thus, it is meaningful for selecting the hybrid functional materials as the SERS substrate to realize reliable quantitative analysis of illegal added drug molecules in complex matrix.

Metal–organic frameworks (MOFs) are considered promising hybrid porous materials consisted of metal ions or clusters and organic ligands through coordination bonds. In recent years, the MOFs materials have exhibited widespread application in catalysis, gas storage, sensing, and drug delivery. In addition to these traditional fields, MOFs materials have received enthusiasm from researchers in SERS applications. Benefiting from the advantages of large surface area, adjustable pore structure, and abundant active sites, MOFs can not only stabilize the nanoparticles, but also effectively capture the target molecules adjacent to the surface of the metal. SERS substrates based on MOFs materials have been constructed [20, 21]. Furthermore, most MOFs materials possess excellent chemical and thermal stability, which provides the possibility of post-modification and post-synthesis. Therefore, the attractive MOFs/nanoparticles composites integrate the preconcentration effect of MOFs and electromagnetic enhancement of nanoparticles to amplify the SERS signal, which will greatly enhance the SERS performance of drug molecules with weak Raman activity and solve the problem in drugs detection. Compared with the classical nanoparticles, these composites are more stable and show higher affinity to drug molecules and improve the sensitivity of SERS determination. Furthermore, the nanoparticles that anchored MOFs substrates display the better SERS enhancement than other MOFs-SERS substrates (nanoparticles embedded or encapsulated in MOFs matrix), whose SERS signal originated from "hot spots" areas is directly enhanced in the interface between MOFs and nanoparticles without any block [22, 23]. So far, there are few reports dedicating to the construction of MOFs combined with metal substrates for determining illegal addition of chemical drugs to healthcare products. Hence, the MOFs materials combined with metal nanoparticles start to be regarded as prospective mode for improving the SERS sensitivity in the determination of drug molecules.

The present study was devoted to fabricating the MOFs-SERS substrate composed of noble metal nanoparticles and MOFs, which could adsorb the analytes, concentrate the drug molecules on electromagnetic enhancement area of AgNPs and improve the affinity of the substrate to drug molecules, further solving the problem of low SERS signal of drug molecules and realizing sensitive analysis of SIL and PIO. The molecular structures of SIL and PIO are shown in Fig. S1. Herein, Fe^{3+} ions as nodes and terephthalic acid (PTA) as a linker were selected to build MOFs, named as MIL101(Fe), and MOFs-AgNPs SERS substrate was obtained via in situ synthesis of AgNPs using tannic acid (TA) as reducing agent. The MOFs with adsorption properties and ultra high surface area gave an opportunity to bring target molecules approaching the surface of AgNPs. The resulting MOFs-AgNPs substrate offered a route for sensitive SIL and PIO analysis. Furthermore, the work reveals high superiority in the determination of drugs in commercial tablets and natural healthcare products.

Experimental

Materials and apparatus

Sodium hydroxide (NaOH), silver nitrate ($AgNO_3$), sodium chloride (NaCl), crystal violet (CV), iron (III) chloride hexahydrate ($FeCl_3{\cdot}6H_2O$), sildenafil (SIL), and pioglitazone hydrochloride (PIO) were supplied from Dingguo (Beijing, China, www.dingguo.com). N,N-dimethylformamide (DMF), terephthalic acid (PTA), and tannic acid (TA) were obtained from Aladdin (http://www.aladdin-e.com). Sucrose, glucose, chitosan, starch, silica fume (SiO_2), H_3BO_3, H_3PO_4, HAC, NaF, KCl, NH_4Cl, $CuCl_2$, and $FeCl_2$ were provided from Chemical Works (Beijing, China, www.beijingchemworks.com). The BR buffer was prepared with a mixture of H_3PO_4 (0.04 mol L^{-1}), H_3BO_3 (0.04 mol L^{-1}), HAc (0.04 mol L^{-1}), and NaOH (0.02 mol L^{-1}) to adjust pH.

Some health products and commercial tablets were obtained at the local pharmacy, including two different types of drinks which are used for anti-fatigue, tablets, and oral liquids with hypoglycemic treatment effects. All chemical reagents were used in the experiment without further refinement. Ultra-pure water (18.2 MΩ) was carried out with through all experiments. The apparatus sections were shown in the Supporting Information.

Preparation of MIL-101(Fe)-AgNPs

MIL-101(Fe) and TA-protected AgNPs synthesis were described in the Supporting Information. MIL-101(Fe)-AgNPs was fabricated via an in situ synthesis strategy [24]. Firstly, MIL-101(Fe) (15 mg) was ultrasonically dissolved in water (9.5 mL), and 0.5 mL of TA solution (40 mg mL^{-1}) was quickly dissolved into the dispersion of MIL-101(Fe) under stirring. Stirred for 20 s, the dark blue product TA-MIL-101(Fe) was obtained by centrifugal separation and washed three times with water for removing the excess TA. The formation of TA-MIL-101(Fe) was due to the complexation between the unsaturated Fe(III) on the MIL-101(Fe) surface and the hydroxyl group in TA, thereby fixing TA to the surface of MOFs. The prepared TA-MIL-101(Fe) was then dispersed in water (9.5 mL), and K_2CO_3 (0.5 mol L^{-1}) was used to adjust the pH value of the solution to 7.5. Finally, the 0.5 mL of $AgNO_3$ (0.2 mol L^{-1}) solution was slowly added to the TA-MIL-101(Fe) dispersion at 600 rpm. During the reaction, TA was used as a reductant to reduce Ag^+ to Ag^0, resulting in the growth of AgNPs on the MOFs surface. All the whole experiment process was maintained under the room temperature. Stirred for 1 h, the black product (MIL-101(Fe)-AgNPs) was collected through centrifugation and washed with water three times. Finally, the as-synthesized MIL-101(Fe)-AgNPs product was dried in the vacuum oven and then dispersed in ultra-pure water (1 mg/mL) for further use.

Preparation of standard and sample solutions

The standard stock solutions with an ultimate concentration of 1.0×10^{-3} mol L^{-1} were made by dissolving SIL and PIO in ultra-pure water and NaOH solution (0.1 mol L^{-1}). Different target concentrations are obtained by diluting the standards. Commercial tablets and natural healthcare products were adopted as real sample solutions for analysis. Commercial tablets (SIL tablet containing 50 mg of SIL per tablet and PIO tablet containing 15 mg of PIO per tablet) were ground into uniform powder in agate mortar. Accurately, 10 mg samples was dissolved in 10 mL methanol and mixed uniformity. The mixture was ultrasonic for 10 min and centrifuged at 4000 rpm for 10 min; then the supernatant was collected for analysis. Natural healthcare products exist in the form of tablets, drinks, and oral liquids. Tablet in healthcare products was ground into uniform powder in agate mortar. Then, 1.0 g samples were accurately weighed, added in 20 mL methanol solution, and then transferred into a 50-mL centrifuge tube. The mixture was ultrasonic for 10 min and centrifuged at 4000 rpm for 10 min. After that, the supernatant was taken for sample analysis. Drinks were used directly without further treatment, and oral liquids were diluted tenfold with ultrapure water for further use.

Determining of SIL and PIO

For SIL, MOFs-AgNPs solution (320 μL), BR buffer (50 μL), and SIL or real sample solution (50 μL) with different concentrations were added into the EP tubes in order. After gentle shaking to mixture the solution, 80 μL of 0.2 M NaCl solution was added in and then left for 5 min at room temperature. After that, the resulting solution was pipetted by capillary tube for SERS detection. Raman spectra were obtained under 532 nm laser excitation. The SERS intensity based on 1402 cm^{-1} of SIL peak was chosen for quantitative analysis. All the experiments were carried out five times.

For PIO, MOFs-AgNPs solution (350 μL), BR buffer (50 μL), and PIO or real sample solution (50 μL) with various concentrations were added in the EP tubes in order. After being mixed, the 50 μL of 0.15 M NaCl was added in and then left for 5 min at room temperature; finally the SERS spectra were collected under 532 nm laser excitation. The SERS intensity located at 628 cm^{-1} of PIO peak was selected for quantitative analysis. All the experiments were carried out five times.

The synthesis route of MOFs-AgNPs and the procedure of SERS detection are depicted in Scheme 1.

Results and discussion

Characterization of MOFs and MOFs-AgNPs

The FT-IR spectra of TA, MOFs, TA-MOFs and as-prepared MOFs-AgNPs substrate are obtained in Fig. S2a. The characteristic broad bands around 1598 and 1394 cm^{-1} of MOFs correspond to the O–C–O symmetric and antisymmetric stretching modes deriving from free ligand. Besides, the apparent peak at 552 cm^{-1} is related to Fe–O bond stretching [25]. These data also proved the successful synthesis of MIL-101(Fe) by metal ions coordinating with free ligand. The detailed peak attribution of TA was placed in the Supporting Information. The peaks appeared at 1685 and 1585 cm^{-1} of TA-MOFs and MOFs-AgNPs are related to the stretching mode of C = O and aromatic C = C bonds of TA. The decrease of the absorption bands at 3000–3500 cm^{-1} in the spectrum of MOFs-AgNPs is owing to the oxidation of

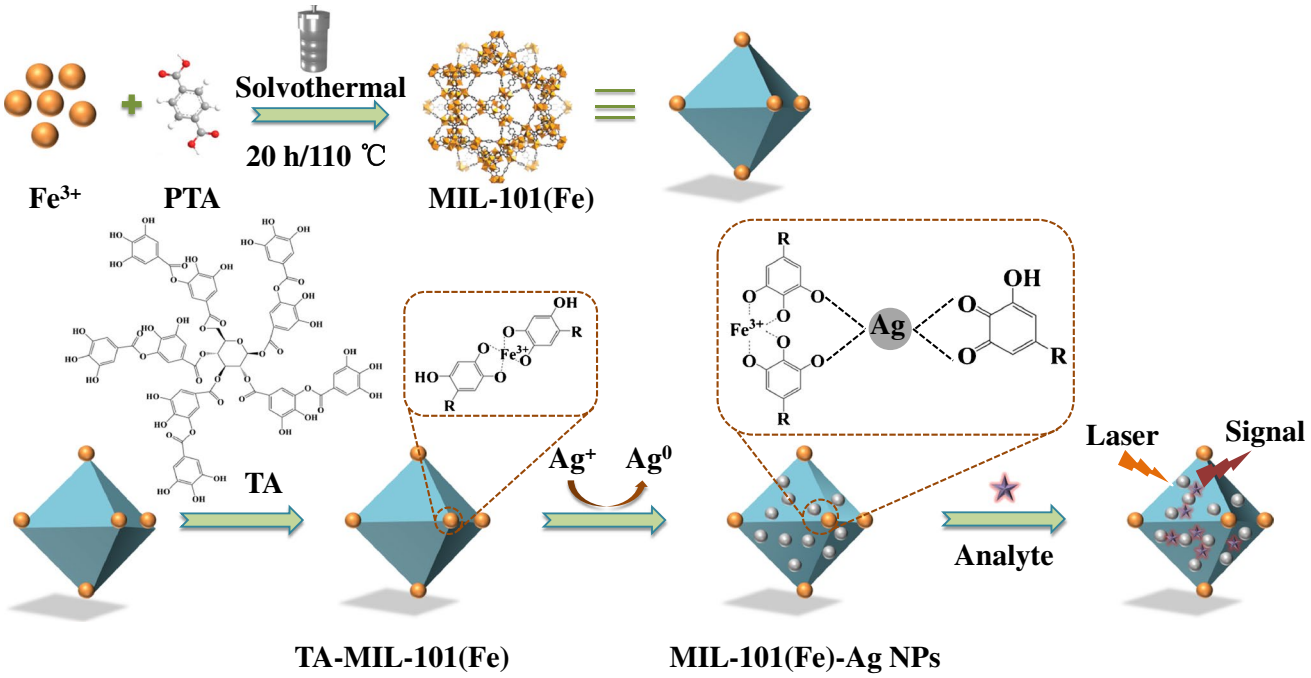

Scheme 1 Schematic illustration of the MOFs-AgNPs synthesis and the SERS detection procedure

the phenolic hydroxyl groups. Taking all together, it could be concluded that π electrons originating from the carbonyl groups of the TA molecules transferred to the free orbitals of the silver ions[26], thereby forming Ag NPs.

The obtained UV–Vis spectra for MOFs and MOFs-AgNPs are presented in Fig. S2b. The peak at about 247 nm of MOFs can be corresponded to the $\pi - \pi^*$ transition of the aromatic C = C bonds in PTA ligand [20]. On the other aspect, it can be seen clearly that the MOFs-AgNPs exhibit a broad absorption in the region of 500–800 nm, which should be assigned to the SPR peak of AgNPs [27].

The XRD patterns of MOFs and MOFs-AgNPs samples are depicted in Fig. S3. The characteristic peaks corresponding to MOFs are observed and are similar to that previously reported [28]. The obvious diffraction peaks of MOFs-AgNPs lying in 38.1°, 44.3°, 64.4°, and 77.5°, attributing to (111), (200), (220), and (311) of Ag (JCPDS no. 65–2871), confirm the existence of Ag in the MOFs-AgNPs composite. The detailed descriptions are given in the Supporting Information.

The morphologies of MOFs and MOFs-AgNPs were characterized by SEM and TEM. The SEM and TEM images (Fig. 1a and 1b) indicate that the prepared MOFs with well-dispersed distribution display a uniform and smooth octahedral structure, with a diameter of about 500 nm. After reducing $AgNO_3$ by TA on the surface of the MOFs, the SEM image of MOFs-AgNPs in Fig. 1c shows that AgNPs are successfully loaded on the surface of MOFs and have no obvious effect on the morphology of MOFs. Meanwhile, well-dispersed AgNPs in MOFs matrix can be clearly demonstrated by its TEM image in Fig. 1d, indicating that MOFs-AgNPs composites have been successfully prepared.

Enhancement factor

To investigate the SERS activity of MOFs-AgNPs composites, crystal violet (CV) was employed as the Raman model analyte for evaluation. The calculated enhancement factor (EF) value reached 4.9×10^5, and the SERS spectra of CV of 10 random collection points were recorded which showed well uniformity and the relative standard deviation (RSD) was 7.2%. The detailed description and experimental process were presented in supporting information (Fig. S4, Fig. S5, and Table S1).

Raman spectra of SIL and PIO

The MOFs-AgNPs substrate was used to determine the SIL and PIO. Figure 2a showed the normal Raman spectrum and SERS spectra of SIL using the different substrates. For the SERS of SIL, the major peaks are located at 1582, 1528, 1488, 1402, 1278, 1235, 928, 818, and 652 cm^{-1}. According to the previous report [15, 16], the SERS bands assignments are listed in Table 1. The SERS peak at 1402 cm^{-1} is on account of the bending vibration of pyrazole ring, C–C stretching mode, and C = C = C bending vibration in benzene ring. The quantitative analysis of SIL is carried out on the basis of the intensity at 1402 cm^{-1} in SERS spectrum.

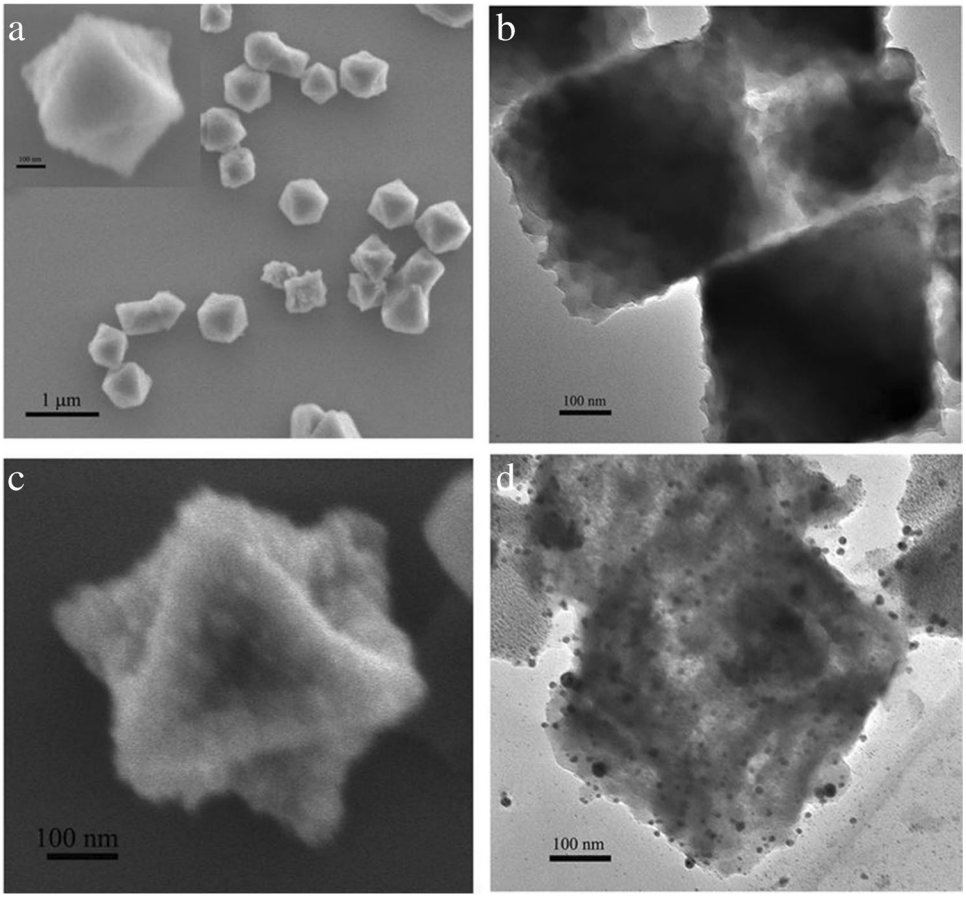

Fig. 1 SEM images of MOFs (**a**) and MOFs-AgNPs (**c**); TEM images of MOFs (**b**) and MOFs-AgNPs (**d**)

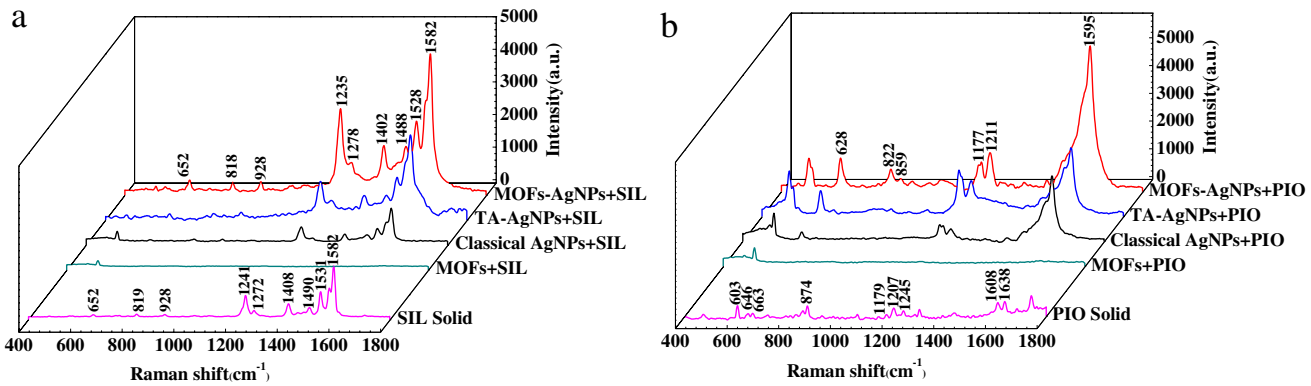

Fig. 2 **a** SERS spectra of 1.0×10^{-4} mol L^{-1} SIL on different SERS substrates and Raman spectrum of pure solid SIL. **b** SERS spectra of 5.0×10^{-6} mol L^{-1} PIO on different SERS substrates and Raman spectrum of pure solid PIO

Compared with the normal Raman spectrum of SIL, a slight Raman shift can be observed in SERS spectra, indicating a strong interaction between SIL and MOFs-AgNPs substrate.

The normal Raman spectrum and SERS spectra of PIO are shown in Fig. 2b. The SERS peaks of PIO are mainly marked at 1595, 1211, 1177, 822, and 628 cm^{-1}. The main band contributions of PIO are shown in Table 1. It can be clear that the peak of PIO at 1608 cm^{-1} is notably enhanced and red-shifts to 1595 cm^{-1}. Besides, the peaks located at 1207 and 1179 cm^{-1} shift to 1211 and 1177 cm^{-1}[29]. The peak at 829 and 859 cm^{-1} from the MOFs-AgNPs substrate is shown in Fig. S6. The shifts of Raman peaks and SERS peaks are related to the interactions between the PIO and AgNPs surface [30]. Among them, the peaks at 628 cm^{-1} originating from the stretching of C–N are used as marker bands for PIO quantitative determination and analysis.

Table 1 Assignment of peaks in SIL and PIO Raman spectra

SIL			PIO		
Solid	SERS	Assignments	Solid	SERS	Assignments
652	652	δ(Pyrimidine), ν(C = O) in pyrimidine	603	628	ν(C–N)
819	818	δ(Benzene ring), ν(C–O) in benzene ring, δ(N = C–N) in pyrimidine	874		ν(C–C), δ(C–C)
928	928	δ(C–C)	1179	1177	δ(C–S), δ(C–H)
1241	1235	δ(C = C–C) in benzene ring	1207	1211	ν(C–N), C–H in-plane bending vibration
1272	1278	δ(C–H), ν(N–H) in pyrimidine ring	1245		C–H in-plane bending vibration
1408	1402	δ(pyrazole ring), ν(C–C), δ(C = C = C) in benzene ring	1608	1595	ν(C = O), ν(C–N)
1490	1488	δ(C–H) in pyrazole pyrimidine ring	1638		ν(C–C), ν(C = O)
1531	1528	ν(C–N) in pyrimidine ring, ν(C–N) in pyrazole ring, δ(C–C) in pyrazole ring			
1582	1582	δ(Benzene ring), δ(C = C = C) in pyrazole ring, ν(C–N) in pyrimidine ring			

ν Stretch vibration, δ bend vibration

Different substrates, including MOFs, classical AgNPs, TA-AgNPs, and MOFs-AgNPs, were used to determine SIL and PIO, respectively. It is obviously found that the MOFs without AgNPs cannot be for the detection of SIL or PIO. Compared with classical AgNPs and TA-AgNPs, the MOFs-AgNPs exhibit a dramatically stronger SERS enhanced effect toward SIL and PIO. This is attributed to the adsorption of SIL or PIO molecules by MOFs, which makes more target molecules concentrating on the SERS hot spots of AgNPs.

The interaction between SIL/PIO and MOFs-AgNPs

The interaction between SIL/PIO and MOFs-AgNPs was analyzed by UV–Vis and FT-IR spectra (Fig. S7 and Fig. S8). These results indicated that the SIL/PIO bound and interacted with AgNPs.

Optimization of experimental condition

To make sure the best SERS enhancement, the experimental conditions for the determination of SIL and PIO, including the pH, the incubation time, and the concentration of NaCl, were optimized. As for the effect of pH, pH = 3.04 and 4.11 were chose as the optimal pH value for the SIL and PIO determination in the further experiment in the Fig. S9, respectively. Figure S10 revealed that 5 min of incubation time achieved the best enhanced effect and 0.2 M and 0.15 M of NaCl were selected as the optimal parameters for determination of SIL or PIO in Fig. S11 and Fig. S12, respectively. The optimization details of experiment conditions are presented in the Supporting Information.

The calibration plots

The Raman spectra of the designed detection method to SIL and PIO with variation concentrations are presented in Fig. 3 at the optimized experiment conditions. It displays that the SERS intensity will apparently increase with increasing of SIL and PIO concentration. For SIL, the satisfactory linear range of SIL obtained at 1402 cm^{-1} is from 1.0×10^{-7} to 1.0×10^{-5} mol L^{-1}, and the linear equation is given as $y = 7.06c + 248.45$ ($R^2 = 0.990$). The limit of detection (LOD) of SIL is calculated to be 4.8×10^{-8} mol L^{-1} based on a signal:noise (S:N = 3). On the other hand, the standard curve for analyzing PIO is given within the range of 8.0×10^{-7}–3.0×10^{-5} mol L^{-1}; the fitted linear equation is presented as $y = 10.98c + 111.90$ and $R^2 = 0.998$. The LOD of PIO is calculated as 1.4×10^{-7} mol L^{-1}. Furthermore, comparison of this work with other strategies is performed in Table 2. Compared to UV and LC-MC/MC, this method exhibited higher sensitivity and wider linear range. The present method using MOFs-AgNPs as a SERS substrate showed lower LOD values than the SERS methods using AgNPs in SIL determination [15, 16], and the determination time only needs no more than 10 min, which can realize the sensitive and rapid determination of SIL and PIO.

Effect of coexisting substances of SIL and PIO

To evaluate the specificity of this proposed strategy, various coexisting interference substances, including metal ions and some drug auxiliary materials such as chitosan, starch, and silica fume (SiO_2), were examined when the concentration of SIL was 8.0×10^{-6} mol L^{-1} and PIO was 5.0×10^{-6} mol L^{-1}. The concentration of the coexisting substances was 8.0×10^{-4} mol L^{-1}. In Fig. 4, these coexisting

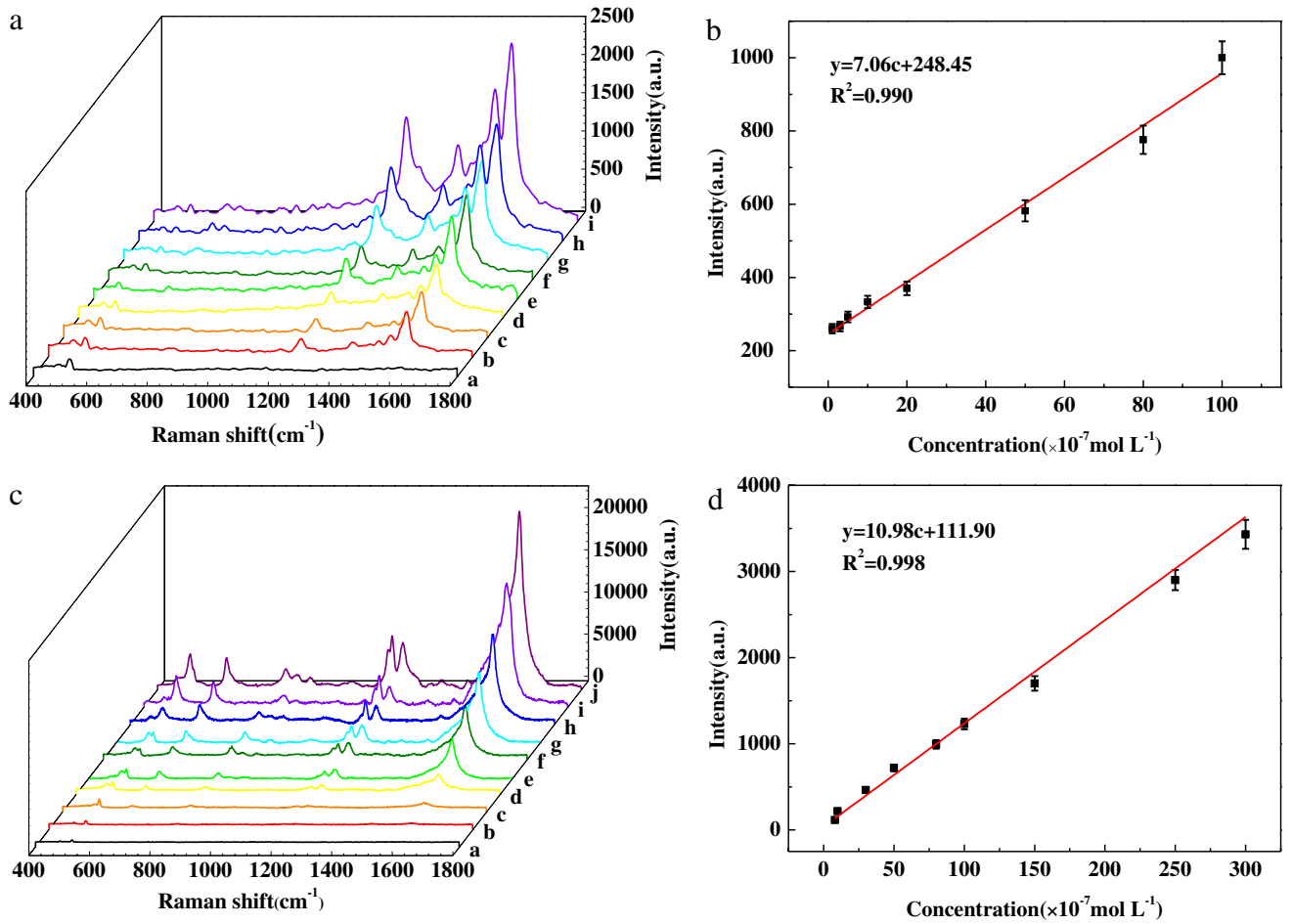

Fig. 3 **a** SERS spectra of SIL with different concentrations ((a–h) 1.0×10^{-7}, 3.0×10^{-7}, 5.0×10^{-7}, 1.0×10^{-6}, 2.0×10^{-6}, 5.0×10^{-6}, 8.0×10^{-6}, 1.0×10^{-5} mol L^{-1}) and **b** the calibration plot of SIL based on SERS intensity at 1402 cm^{-1}. **c** SERS spectra of PIO with different concentrations ((a–i) 8.0×10^{-7}, 1.0×10^{-6}, 3.0×10^{-6}, 5.0×10^{-6}, 8.0×10^{-6}, 1.0×10^{-5}, 1.5×10^{-5}, 2.5×10^{-5}, 3.0×10^{-5} mol L^{-1}) and **d** the calibration plot of PIO based on SERS intensity at 628 cm^{-1}

Table 2 Comparison of other methods with the current method for the determination of SIL and PIO

Method		Linear range (mol L^{-1})	LOD (mol L^{-1})	Ref
SERS	SIL	1.0×10^{-7}–1.0×10^{-5}	4.8×10^{-8}	This work
	PIO	8.0×10^{-7}–3.0×10^{-5}	1.4×10^{-7}	
SERS	SIL	2.1×10^{-6}–2.1×10^{-5}	2.1×10^{-6}	[15]
		2.1×10^{-7}–2.1×10^{-5}	2.1×10^{-7}	[16]
	PIO	5.0×10^{-9}–1.0×10^{-3}	1.0×10^{-9}	[17]
Electrochemistry	SIL	9.0×10^{-9}–5.0×10^{-7}	—	[5]
	PIO	1.0×10^{-6}–1.0×10^{-2}	—	[6]
UV	SIL	—	—	
	PIO	2.5×10^{-5}–2.3×10^{-4}	—	[7]
HPLC	SIL	1.0×10^{-8}–5.0×10^{-7}	3.1×10^{-9}	[8]
	PIO	1.3×10^{-6}–1.8×10^{-5}	3.3×10^{-7}	[9]
Fluorescence	SIL	—	—	
	PIO	1.3×10^{-7}–3.3×10^{-6}	4.1×10^{-9}	[12]
LC-MC	SIL	2.1×10^{-9}–2.1×10^{-6}	2.1×10^{-9}	[13]
LC-MC/MC	PIO	3.1×10^{-5}–6.2×10^{-3}	—	[14]

Table 3 Analytical results of SIL and PIO in commercial tablets and natural healthcare products ($n = 5$)

		Added ($\times 10^{-7}$ mol L^{-1})	Found ($\times 10^{-7}$ mol L^{-1})	Recovery (%)	RSD (%)
SIL	Commercial tablet	6.4	6.7	104.7	3.6
		64.0	62.0	96.9	4.1
		80.0	82.6	103.2	3.9
	Drink 1	6.4	6.6	103.1	3.3
		64.0	69.1	108.0	3.0
		80.0	78.6	98.3	2.7
	Drink 2	6.4	6.0	93.8	3.9
		64.0	63.5	99.2	3.4
		80.0	81.7	102.1	3.6
PIO	Commercial tablet	10.0	10.3	102.5	2.2
		100.0	94.9	94.9	3.3
		200.0	204.2	102.1	4.0
	Tablet in healthcare product	10.0	9.3	93.0	3.0
		100.0	96.4	96.4	3.2
		200.0	191.9	96.0	2.9
	Oral liquid	10.0	10.4	104.0	4.2
		100.0	98.5	98.5	2.8
		200.0	196.6	98.3	3.5

substances have little interference to the SIL or PIO SERS, with maximum relative errors less than 5.0%.

Sample analysis

For validating the accuracy of the designed SERS method, the SIL (50 mg per tablet) and PIO (15 mg per tablet) in commercial tablets samples were determined compared with UV–Vis method. The results showed that the amounts of SIL and PIO per tablet were 52.7 and 14.1 mg by SERS method and the RSD were 3.8 and 3.2, respectively. The contents of SIL and PIO per tablet were 51.5 and 14.7 mg with RSD of 2.9 and 3.4 by UV–Vis method, respectively, which was not significantly different from SERS method. The recoveries studies of three concentrations of SIL and PIO standard solutions were performed in commercial tablets samples. As illustrated in Table 3, the recoveries obtained were 94.9–104.7% with RSD of 2.2–4.1%. These results demonstrated that the designed SERS method was suitable for the analysis of practical samples.

The established method was also applied to analyze whether SIL/PIO had been illegally added in natural health products. The healthcare products were analyzed, including two different types of anti-fatigue drinks, hypoglycemic tablets and oral liquids. SIL or PIO had not been found in their respective natural healthcare products. For verifying the practice application of this assay platform, certain concentrations of SIL or PIO standard solutions were separately spiked into the respective real samples, and the Table 3 shows the experiment results. The recoveries of SIL obtained were 93.8–108.0% and RSD varied from 2.7 to 3.9%. As for PIO, the recoveries were 93.0–104.0% and RSD varied from 2.8 to 4.2%. The results indicated that the proposed SERS approach based on the MOFs-AgNPs substrate had well applicability. Some organic species and drug molecules with Raman activity or Raman signal in the real sample may interfere with the determination of SIL and PIO. However, if the peak positions of these molecules in SERS spectrum are different from the analytes, the determination will not be interfered, and qualitative analysis and quantitative analysis may be achieved simultaneously through SERS "fingerprint" properties.

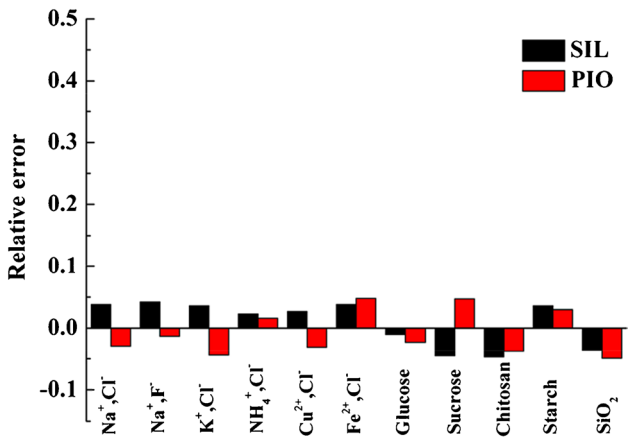

Fig. 4 Effect of coexisting substances

Conclusions

In this work, MOFs-AgNPs composites are successfully constructed as an efficient SERS substrate. Taking advantage of the adsorption properties and large surface area of MOFs, this new type of SERS substrates can force the target molecules closer to the SERS-active sites of AgNPs. The as-prepared MOFs-AgNPs substrate exhibits superior SERS performance than classical AgNPs, and the successful quantitative determination of SIL and PIO suggests that the MOFs-AgNPs substrate has a great application in SERS analysis areas. Meanwhile, this established analytical method can be utilized to analyze the SIL and PIO in commercial tablets and healthcare products with satisfactory recovery. Some other drug molecules with Raman activity or Raman signal in the real sample may be interfered with the determination of analyte. This work shows great potential of MOFs-AgNPs substrate in other drug molecules testing in illegally added healthcare products.

Supplementary Information The online version contains supplementary material available at https://doi.org/10.1007/s00604-021-05008-4.

Funding The work was supported by the Science-Technology Development Project of Jilin Province of China (No. 20170101174JC) and the National Natural Science Foundation (Grant Nos. 21773080, 21711540292, and 21773079) of the People's Republic of China.

Declarations

Conflict of interest The authors declare no competing interests.

References

1. Singh S, Prasad B, Savaliya AA, Shah RP, Gohil VM, Kaur A (2009) Strategies for characterizing sildenafil, vardenafil, tadalafil and their analogues in herbal dietary supplements, and detecting counterfeit products containing these drugs. TrAC Trends Anal Chem 28(1):13–28
2. Huang AC, Kuei-Ying Y, Cheng YY, Navneet D, Allen C, Tung-Hu T (2018) Investigation of interactive activity of electro-acupuncture on pharmacokinetics of sildenafil and their synergistic effect on penile blood flow in rats. Int J Mol Sci 19(8):2153
3. Chen Y, Liang D, Ling L, Ma J, Geng X, Xun Y, Liu Z, Xin S (2017) Cancer risk of sulfonylureas in patients with type 2 diabetes mellitus: A systematic review. J. Diabetes 9(5):482–494
4. Pavasini R, Camici PG, Crea F, Danchin N, Fox K, Manolis AJ, Marzilli M, Rosano GMC, Lopez-Sendon JL, Pinto F, Balla C, Ferrari R (2019) Anti-anginal drugs: systematic review and clinical implications. Int J Cardiol 283:55–63
5. Berzas JJ, Rodriguez J, Castañeda G, Villaseñor MJ (2000) Voltammetric behavior of sildenafil citrate (Viagra) using square wave and adsorptive stripping square wave techniques: Determination in pharmaceutical products. Anal Chim Acta 417(2):143–148
6. Mostafa GA, Al-Majed A (2008) Characteristics of new composite- and classical potentiometric sensors for the determination of pioglitazone in some pharmaceutical formulations. J Pharm Biomed Anal 48(1):57–61
7. Yilmaz E, Ulusoy Hİ, Demir Ö, Soylak M (2018) A new magnetic nanodiamond/graphene oxide hybrid (Fe_3O_4@ND@GO) material for pre-concentration and sensitive determination of sildenafil in alleged herbal aphrodisiacs by HPLC-DAD system. J Chromatogr B: Biomed Sci Appl 1084:113–121
8. Mohamed AM, Ezzat AH, Mohamed HM, Abdel-Sattar KN (2018) High performance liquid chromatographic estimation of pioglitazone hydrochloride and losartan potassium. Main Group Chem 17(3):247–256
9. Hegazy MA, El-Ghobashy MR, Yehia AM, Mostafa AA (2009) Simultaneous determination of metformin hydrochloride and pioglitazone hydrochloride in binary mixture and in their ternary mixture with pioglitazone acid degradate using spectrophotometric and chemometric methods. Drug Test Anal 1(7):339–349
10. Zhu QX, Cao YB, Cao YY, Chai YF, Lu F (2014) Rapid on-site TLC-SERS detection of four antidiabetes drugs used as adulterants in botanical dietary supplements. Anal Bioanal Chem 406(7):1877–1884
11. Minh DTC, Huyen NTT, Anh NTK, Ha PTT (2019) Detection of sildenafil adulterated in herbal products using thin layer chromatography combined with surface enhanced Raman spectroscopy: "Double coffee-ring effect" based enhancement. J Pharm Biomed Anal 174:340–347
12. Alarfaj NA, Al-Abdulkareem EA, Aly FA (2011) Spectrofluorimetric determination of pioglitazone hydrochloride and glimepiride in their formulations and biological fluids. Asian J Chem 23(8):3441–3444
13. Tanaka S, Uchida S, Hakamata A, Miyakawa S, Odagiri K, Inui N, Watanabe H, Namiki N (2020) Simultaneous LC-MS analysis of plasma concentrations of sildenafil, tadalafil, bosentan, ambrisentan, and macitentan in patients with pulmonary arterial hypertension. Pharmazie 75(6):236–239
14. Praveen DSS, Asha S, Kumar PR (2019) Simple and rapid liquid chromatography-tandem mass spectrometric (LC-MS/MS) method for the simultaneous determination of pioglitazone and glimepiride in human plasma. Curr Trends Biotechnol Pharm 13(2):190–198
15. Zhao H, Hasi WLJ, Bao L, Han SQGW, Sha XY, Sun J, Lou XT, Lin DY, Lv ZW (2017) Rapid detection of sildenafil drugs in liquid nutraceuticals based on surface-enhanced Raman spectroscopy technology. Chin J Chem 35(10):1522–1528
16. Lin L, Qu FF, Nie PC, Zhang H, Chu BQ, He Y (2019) Rapid and Qqantitative determination of sildenafil in cocktail based on surface enhanced Raman spectroscopy. Molecules 24(9):1790
17. Liu CY, Xu XH, Wang CD, Qiu GY, Ye WC, Li YM, Wang DG (2020) ZnO/Ag nanorods as a prominent SERS substrate contributed by synergistic charge transfer effect for simultaneous detection of oral antidiabetic drugs pioglitazone and phenformin. Sens Actuators B Chem 307:127634
18. Wu JW, Ma H, Bu XF, Ma C, Zhu L, Hao BQ, Zhao B, Tian Y (2019) SERS determination of the antihypertensive drugs prazosin and losartan by using silver nanoparticles coated with β-cyclodextrin. Microchim Acta 186(12):1–10
19. Kreno LE, Greeneltch NG, Farha OK, Hupp JT, Van Duyne RP (2014) SERS of molecules that do not adsorb on Ag surfaces: a metal-organic framework-based functionalization strategy. Analyst 139(16):4073–4080
20. Xuan T, Gao Y, Cai YZ, Guo XY, Wen Y, Yang HF (2019) Fabrication and characterization of the stable Ag-Au-metal-organic-frameworks: an application for sensitive detection of thiabendazole. Sens Actuators B Chem 293:289–295
21. Wu LL, Pu HB, Huang LJ, Sun DW (2020) Plasmonic nanoparticles on metal-organic framework: A versatile SERS platform for

adsorptive detection of new coccine and orange II dyes in food. Food Chemistry 328:127105
22. Lai HS, Li GK, Xu FG, Zhang ZM (2020) Metal-organic frameworks: opportunities and challenges for surface-enhanced Raman scattering-a review. J Mater Chem C 8(9):2952–2963
23. Fu JT, Lai HS, Zhang ZM, Li GK (2021) UiO-66 metal-organic frameworks/gold nanoparticles based substrates for SERS analysis of food samples. Anal. Chim. Acta 116:338464
24. Jiang ZW, Gao PF, Yang L, Huang CZ, Li YF (2015) Facile in situ synthesis of silver nanoparticles on the surface of metal-organic framework for ultrasensitive surface-enhanced Raman scattering detection of dopamine. Anal Chem 87(24):12177–12182
25. Taylor-Pashow KM, Della Rocca J, Xie ZG, Tran S, Lin WB (2009) Postsynthetic modifications of iron-carboxylate nanoscale metal-organic frameworks for imaging and drug delivery. J Am Chem Soc 131(40):14261–14263
26. Veisi H, Moradi SB, Saljooqi A, Safarimehr P (2019) Silver nanoparticle-decorated on tannic acid-modified magnetite nanoparticles (Fe_3O_4@TA/Ag) for highly active catalytic reduction of 4-nitrophenol, Rhodamine B and Methylene blue. Mater Sci Eng C 100:445–452
27. Chen LM, Liu YN (2011) Surface-enhanced Raman detection of melamine on silver-nanoparticle-decorated silver/carbon nanospheres: effect of metal ions. ACS Appl Mater Interfaces 3(8):3091–3096
28. Hu H, Zhang HX, Chen YJ, Qu HS (2019) Enhanced photocatalysis using metal-organic framework MIL-101(Fe) for organophosphate degradation in water. Environ Sci Pollut Res 26(24):24720–24732
29. Rajesh S, Gunasekaran S, Rajesh P (2018) Vibrational and molecular structural investigations of pioglitazone-combined study of experimental and quantum chemical calculations (density functional theory). Int J ChemTech Res 11(10):111–125
30. Wang KQ, Sun DW, Pu HB, Wei QY (2019) Surface-enhanced Raman scattering of core-shell Au@Ag nanoparticles aggregates for rapid detection of difenoconazole in grapes. Talanta 191:449–456